A Sensitivity Analysis Methodology For Rule-Based Stochastic Chemical Systems

Erika M. Herrera Machado[1,2], Jakob L. Andersen[1], Rolf Fagerberg[1], and Daniel Merkle[3,1]

[1]Department of Mathematics and Computer Science, University of Southern Denmark, Odense, Denmark
`{jlandersen,rolf,machado}@imada.sdu.dk`
[2]Faculty of Mathematics and Computer Science, Friedrich Schiller University Jena, Jena, Germany
[3]Faculty of Technology, Bielefeld University, Bielefeld, Germany `daniel.merkle@uni-bielefeld.de`

September 23, 2025

Abstract

In this study, we introduce a sensitivity analysis methodology for stochastic systems in chemistry, where dynamics are often governed by random processes. Our approach is based on gradient estimation via finite differences, averaging simulation outcomes, and analyzing variability under intrinsic noise. We characterize gradient uncertainty as an angular range within which all plausible gradient directions are expected to lie. This uncertainty measure adaptively guides the number of simulations performed for each nominal-perturbation pair of points in order to minimize unnecessary computations while maintaining robustness.

Systematically exploring a range of parameter values across the parameter space, rather than focusing on a single value, allows us to identify not only sensitive parameters but also regions of parameter space associated with different levels of sensitivity. These results are visualized through vector field plots to offer an intuitive representation of local sensitivity across parameter space. Additionally, global sensitivity coefficients are computed to capture overall trends.

Flexibility regarding the choice of output observable measures is another key feature of our method: while traditional sensitivity analyses often focus on species concentrations, our framework allows for the definition of a large range of problem-specific observables. This makes it broadly applicable in diverse chemical and biochemical scenarios. We demonstrate our approach on two systems: classical Michaelis-Menten kinetics and a rule-based model of the formose reaction, using the cheminformatics software MØD for Gillespie-based stochastic simulations.

1 Introduction

Mathematical modeling has become increasingly important for understanding biological and chemical systems. These models not only serve as predictive tools but also offer valuable insights into the mechanisms underlying observed behaviors. Common model parameters include reaction rates, initial conditions, activation energies, and thermodynamic constants. Estimating the values of such parameters is often subject to uncertainty [32, 29].

Sensitivity analysis is the study of how input parameters influence the model output. If small changes in a parameter result in significant variations in the outcome, the model is considered sensitive to that parameter. The application of sensitivity analysis in chemical and biochemical systems serves multiple purposes, including: i) identifying the key parameters in the model, ii) understanding how changes in input values influence the model output, iii) assessing the robustness of the model, iv) simplifying the model by removing parameters of low impact, and v) inferring the

model's output in the vicinity of a given point without the need to rerun the experiment [32, 29, 28, 18, 36]. We elaborate on the background of the field in section Related Work.

For modeling the time evolution of chemical systems, a stochastic approach is often more suitable than a deterministic one, especially for complex systems, systems prone to fluctuations, or systems where discreteness and stochasticity play important roles [29, 36, 5, 17]. However, the uncertainty and noise present in stochastic systems add additional challenges to sensitivity analysis. Section Simulation of Stochastic Chemical Systems briefly introduces stochastic chemical systems and modeling formalisms.

Stochastic modeling is often well-suited to rule-based systems in certain contexts. Rule-based generative modeling is a paradigm that addresses the potential combinatorial complexity associated with these chemical systems. By representing molecules as agents and interactions as rules that describe how local patterns should be modified, it is possible to avoid the need for enumerating all possible reactions between all possible molecular species [14, 6]. In other words, rule-based modeling offers a powerful simplification of complex biochemical systems by describing them by a concise set of rules rather than an extensive set of specific reactions. Furthermore, being generative, the system can be initialized with a small number of molecular species instead of a comprehensive list of possible species. This abstraction is especially advantageous for sensitivity analysis: by naturally reducing the dimensionality of the parameter space, rule-based models make the analysis more tractable, both computationally and conceptually. In the context of our approach, this allows for a more efficient exploration of system behavior and facilitates the visualization of the sensitivity across the parameter space. One computational framework working in this paradigm is the software package MØD [2], which approaches rule-based generative chemistry via graph grammars where atoms are explicitly represented. MØD contains a module for performing Gillespie-based stochastic simulation [21], which forms the vehicle by which we display our methodology.

In this work, we propose a sensitivity analysis methodology for discrete stochastic systems. A major strength of our proposal is its flexibility in defining the subject of the analysis, which may be any observable that the user can define on the simulation trace[1]. As examples, an observable can be the number of molecular species A present at the end, the time elapsed before molecular species B appears for the first time, the number of times reaction R took place before reaction S first occurred, or the average number of carbons per molecule in the molecular population at the end. Once an objective has been chosen, we then average its value over repeated runs of the stochastic simulation to account for intrinsic noise. The next ingredient is to estimate the gradient of the output observable function using finite differences. We do that not just at a single nominal point, but across a set of values for each parameter. This exploration of a range of values allows us to detect not only sensitive parameters but also specific regions associated with high or low sensitivity.

A key feature of our method is that the number of repetitions of each simulation is chosen in a structured manner that aims at balancing computational time with precision achieved at each point in the parameter space. For this, we leverage statistical concepts such as the Central Limit Theorem for quantifying the uncertainty of the estimated gradient as an angular uncertainty of the gradient's direction. Since this uncertainty varies for each nominal-perturbation pair of points, we adapt the number of simulations accordingly to ensure consistent precision. Finite difference approaches in the literature have proven to be effective [29, 36, 18, 30]. However, some works argue against it due to the excessive number of function evaluations required and its unreliability in the presence of noise [27, 32]. Working with low-dimensional parameter spaces in rule-based systems and employing a systematic and adaptive method for result averaging help us mitigate these issues in our approach.

---

[1]Simulation trace: a record of the time evolution of a system during a single simulation run.

Additionally, we present results as a series of vector fields over the parameter space, offering a more interpretable view compared to other sensitivity analysis techniques. These visualizations help identify directions within the input space for improving robustness or optimizing observable values, and capture the combined effects of multiple parameters. We also calculate global sensitivity coefficients for each parameter to quantify their overall importance and impact on the model.

The rest of this paper is structured as follows. In section Simulation of Stochastic Chemical Systems, we introduce stochastic chemical systems and modeling formalisms. The section Related Work provides a review of existing approaches for deterministic and stochastic modeling. In section Methodology, we describe our approach in detail. The section Application Examples illustrates this methodology using the well-known Michaelis-Menten kinetics and a rule-based model for formose chemistry. Finally, section Conclusion closes the paper by summarizing the work we have carried out.

2   Simulation of Stochastic Chemical Systems

Stochastic chemical systems describe the behavior of chemical reactions where the evolution of molecular populations is inherently random. Such systems are particularly prominent in biological and biochemical contexts, where molecular populations can be small, and random fluctuations play a significant role in system behavior. For example, gene expression, cellular signaling, and metabolic pathways often exhibit stochastic dynamics that cannot be captured by deterministic models [18, 30, 19].

Unlike deterministic models, which predict exact outcomes based on initial conditions, stochastic models account for this probabilistic nature of molecular interactions [29, 36, 5, 17]. Stochastic chemical systems are typically modeled as continuous-time Markov processes [18, 30, 19] where the state of the system is represented by a vector of non-negative integers corresponding to the number of molecules of each species. The system evolves through discrete reaction events, each characterized by a propensity function that defines the probability of a reaction occurring in a given time interval. The evolution of the system's probability distribution over time is described by the Chemical Master Equation (CME), a differential equation that describes the time-dependent probability of the system being at each possible state. The CME models stochastic dynamics of reacting systems accounting for the inherent randomness in molecular events.

However, the CME is often intractable to solve analytically. Instead, numerical trajectories of the system can be efficiently generated using stochastic simulation algorithms (SSA), such as the Direct Method introduced by Gillespie [17], in which for each reaction r a propensity function is defined which measures the probability that r will occur in the system in the next time interval $[t, t+dt)$. For systems with complex reaction mechanisms involving numerous molecular interactions, rule-based modeling provides a powerful alternative to explicitly enumerating all possible reactions [14, 9], as described in section Introduction. Finally, generative, rule-based stochastic simulation approaches, such as the one implemented in MØD [2, 21], use reaction rules to dynamically generate the relevant parts of the underlying reaction networks during the simulation, capturing the stochastic evolution of molecular populations while significantly reducing computational complexity. This is particularly useful for modeling biochemical networks with large numbers of interacting species, where traditional reaction-based representations become infeasible.

3 Related Work

3.1 Previous Work on Sensitivity Analysis in Chemical Systems

In the context of chemical kinetics, categorizing methodologies is a multidimensional task. In this paper, we consider the following dimensions for discussing and categorizing existing work:

- Scope: global or local.

- Modeling formalism: traditional ODE system, or Gillespie SSA-based.

- Source of randomness: the input variable values, or intrinsic stochastic effects.

- Output observable of the analysis: species concentrations are the standard, but other interesting measures can be considered.

- Time handling: as a variable, or fixed in advance.

In the following, we highlight mainly the works that provide the necessary context for our study, in order to illustrate how it fits into this broad and evolving field. The selected citations are organized to reflect the historical trend of chemical kinetics formalisms from deterministic ODE-based models to the adoption of Gillespie SSA-based techniques for stochastic systems.

3.1.1 Deterministic Modeling

Traditional sensitivity analysis is applied to continuous deterministic systems. The evolution of a spatially homogeneous chemical system is typically modeled by the ordinary differential equation system

$$\frac{d\mathbf{c}}{dt} = \mathbf{f}(\mathbf{c}, \mathbf{x}, t), \quad \mathbf{c}(0) = \mathbf{c}^0, \tag{1}$$

where $\mathbf{c}$ is the vector of species concentrations, $\mathbf{x}$ is the vector of system parameters, t represents time, and $\mathbf{c}^0$ is the vector of initial conditions.

Local methods generally produce sensitivity coefficients representing parametric gradients at single points in the parameter space [29, 36, 24]. We want to highlight two methods that are regarded as the simplest and likely the most intuitive in this category. The first one, assuming Eq. 1 is solved for various sets of parameter values, consists of calculating local first-order sensitivity coefficients with respect to the jth parameter x_j, defined as

$$\frac{\partial \mathbf{c}(t)}{\partial x_j}. \tag{2}$$

These coefficients inform us about the effect of small variations in the parameter around its nominal value on $\mathbf{c}(t)$. The rest of parameters are fixed, therefore this approach falls in the class of the One-at-a-Time (OAT) methods. Higher-order coefficients can be obtained from the Taylor series expansion. Finite differences are commonly used to approximate these gradients [29, 36], this approach is also known as brute-force sensitivity analysis. The next classical method is referred to as the direct method, as it involves the solution of the differential equations that govern the sensitivity coefficients. In other words, directly differentiating Eq. 1 with respect to x_j we obtain

$$\frac{d}{dt}\frac{\partial \mathbf{c}}{\partial x_j} = \mathbf{J}(t)\frac{\partial \mathbf{c}}{\partial x_j} + \frac{\partial \mathbf{f}(t)}{\partial x_j}, \tag{3}$$

where $\mathbf{J}(t) = \frac{\partial \mathbf{f}}{\partial \mathbf{c}}$ and the initial condition for $\frac{\partial \mathbf{c}}{\partial x_j}$ is a zero vector. We refer to Refs. [29, 36] for a more comprehensive review of local methods and solutions to the equations discussed.

Global methods are useful when one considers large variations of the system parameters. As pointed out in [29], the most intuitive approach would consist of generating a solution surface in the parameter space by calculating solutions of Eq. 1 for different parameter values. However, this task can become unfeasible for a large number of species and parameters. Two of the foundational global methods that we will briefly introduce here rely on the assumption that the parameter vector $\mathbf{x}$ is a random vector with known (or somehow estimable) probability distribution. The first one of them is proposed by [10], where the task of sensitivity analysis consists of determining the probability distribution p of the concentrations $\mathbf{c}(t)$, given the probability density function (pdf) of the parameters. They achieve this by solving the partial differential equation

$$\frac{\partial p}{\partial t} = \nabla(Fp), \tag{4}$$

where $F = \frac{d\mathbf{z}}{dt}$, with $\mathbf{z}$ being the joint vector of concentrations and parameters. In this context, the authors define stochastic sensitivity coefficients as $\frac{\partial p}{\partial x_j}$. The next global method is the Fourier amplitude sensitivity test (FAST) [11, 12]. Here, the model parameters are expressed as periodic functions of a search variable s. This is done using transformations of the form:

$$x_j = G_j \left(\sin\left(\omega_j s\right)\right) \tag{5}$$

This reformulation converts a multidimensional integral over the parameters into a one-dimensional integral over s. The transformation functions G_j are uniquely determined (see references for details). By selecting appropriate integer frequencies ω_j, the model outputs become 2π-periodic functions of s and can be analyzed using Fourier methods.

Other traditional methods include: i) Monte Carlo methods, where parameter values are generated based on the probability distributions, then solving the system and analyzing results statistically [32], ii) the Morris screening method [25, 32, 37] for identifying influential parameters, and iii) variance-based methods such as Sobol indices [35], which quantify the contribution of input parameters to output variability.

The methods presented above are historically among the foundational ones in the field of sensitivity analysis for studying chemical kinetics. We have already categorized them along the local/global dimension and now look at the other categorical dimensions. For all these methods, their modeling formalism is the traditional deterministic view of chemical kinetics where species concentrations over time are modeled through a set of ODEs. The term "stochastic" earlier did occur, but then generally [4, 23] referred to uncertainty in the parameter vector values, i.e., how variability in the parameter vector $\mathbf{x}$ generates uncertainty in the concentration vector $\mathbf{c}(t)$. However, some works already approached stochastic systems where the randomness comes instead from the molecular events, especially in systems with a small amount of molecules. Stochastic differential equations were still a standard to handle these cases, usually by incorporating noise terms. Regarding the output of the analysis, the general tendency was the concentrations of the molecular species. In the methods presented above, time has been handled as an explicit independent variable to analyze the system's evolution over time.

3.1.2 Stochastic Modeling

The next block of citations focuses on those where Gillespie's SSA-based techniques are employed to model stochastic kinetics and where the source of randomness comes from the internal stochastic

effects due to the probabilistic nature of biochemical reactions, rather than variability in parameter values themselves.

In [18], the authors present a methodology for parametric sensitivity analysis based on density function sensitivity for discrete stochastic systems, modeled by CMEs. Deriving sensitivity coefficients directly from the CME is complex, so the authors estimate the pdf of the system by generating SSA realizations of its states over time. They then derive sensitivity measures employing finite differences and the Fisher Information Matrix (FIM) to analyze how changes in the input parameters affect the pdf. Their analysis is applied to the Schlögl model and a synthetic genetic toggle-switch model. A discussion between stochastic and deterministic analyses is provided as well.

Ref. [15] explores both local and global sensitivity analysis methods applied to biochemical models, comparing deterministic and stochastic approaches to SA. The analysis output is species concentrations evaluated at specific fixed time points. Local OAT methods are adapted for stochastic models using SSA, in one approach averaging simulation outputs, and in another employing histogram distances to quantify differences in the output distributions. For global analysis, a variance-based method is discussed, which also utilizes histogram distances. They analyze the Schlögl model and the MAPK signaling pathway.

In [30], the authors investigate sensitivity via finite perturbations in stochastic chemical systems using SSA simulations. They introduce two methods for reducing the variance in the statistical estimator described in [18]: the Common Random Numbers (CRN) and Common Reaction Path (CRP). CRN reduces variance by introducing dependence between perturbed and unperturbed simulations through shared random number streams. CRP extends this approach by ensuring tighter coupling between reaction paths via independent streams per reaction channel, leading to more continuous perturbations and lower variance compared to CRN. Comparatively, CRP outperforms CRN in terms of variance reduction and estimator efficiency.

In [34], SPSens is introduced as a software package for efficient computation in stochastic parameter sensitivity analysis of biochemical reaction networks. The software estimates sensitivity coefficients related to the expected value of the system output to account for the stochastic nature of the systems considered. These coefficients are estimated using SSA realizations. Several sensitivity algorithms are implemented in C, including the finite difference approach and the aforementioned CRN and CRP, among others. It also includes variance reduction methods for improved precision.

Ref. [13] presents a numerical methodology for parameter sensitivity analysis in catalytic reaction networks, focusing on how parameters influence the probability distribution of the model output. Their sensitivity measure is based on the one developed by [18], with the difference that here, the sensitivity coefficients, rather than referring to all the output variables described by a single probability distribution, analyze sensitivity with respect to custom individual variables. They explore a range of parameter values rather than focusing on a single nominal value, which results in a more informative sensitivity assessment. SSA is used to simulate the stochastic dynamics, and a kernel method approximates the pdfs of the output variables. The parameters are ranked based on their influence.

The authors in [26] review established finite-difference estimators for sensitivity analysis, such as the previously mentioned CRP and CRN from [30], and the Coupled Finite Difference (CFD) method by [3]. They propose a novel strategy for application to stiff systems, coupling paths that are obtained via tau-leaping, and show significant improvement in efficiency and similar accuracy to the CFD method.

In the domain of sensitivity analysis for stochastic chemical/biochemical systems, the cited works show that the use of Gillespie's SSA to account for intrinsic stochastic effects is by now standard practice. These approaches often focus on estimating pdfs or sensitivity coefficients to understand the system behavior under slight perturbations in the input parameter values, which are generally

fixed in advance. The scope of the reviewed papers is primarily local, as they analyze effects around fixed nominal parameter values, although some studies explore a broad range of parameter values as in [13]. Regarding the observables of the analysis, species concentrations are predominant. Time handling is varied; some approaches conduct the analyses at fixed, predetermined time points, while other methods treat time as a variable, where sensitivity is assessed over entire time trajectories.

The reviewed methods significantly contribute to understanding sensitivity in stochastic chemical kinetics. However, some often occurring limitations include: relying on a fixed nominal value per parameter, rather than a range of values; focusing predominantly on species concentrations as observables; or fixing in advance the number of simulations required. In our approach, we overcome these limitations by proposing a methodology that incorporates intrinsic stochasticity via Gillespie simulations and provides a geometric characterization of gradient uncertainty. The parameter space is explored for a range of values for each individual parameter, adapting the number of simulations based on the precision of the gradient estimate. Additionally, the choice of output observables is very flexible. We aim to offer an efficient, robust, and adaptable framework for sensitivity analysis of chemical systems where results are intuitive and visual.

4   Methodology

4.1   Overview

We consider sensitivity analysis of a stochastic model with n real-valued input parameters of interest. This could for instance be a chemical reaction network with n of the reaction rate constants as parameters. For sensitivity analysis to be meaningful, it is important to explore a representative range of values for each parameter [13], since a system's observable may exhibit low sensitivity to changes in a parameter around one reference value, but high sensitivity around another. We therefore allow the user to define a subset $X \subseteq \mathbb{R}^n$ of the n-dimensional Euclidean parameter space, which will be the parameter values studied. The observable can be any user-defined value computable from the simulation trace (i.e., the sequence of system states and events during one simulation).

We make the assumption on the stochastic system and the observable chosen that if the same simulation for a fixed parameter vector $\mathbf{x} \in X$ is repeated many times, the average of the observed values converges to some value. Thinking of this value as a function of $\mathbf{x}$, our goal will be to estimate the gradient of that function. For this, we use the method of finite differences, i.e. for a given nominal point $\mathbf{x} \in X$, perturb one of its components slightly, and find the average observable value of repeated simulations on both $\mathbf{x}$ and on the perturbed point. Then use these averages to find an approximation to the corresponding component of the gradient vector.

A key element of our methodology is to choose the number of repetitions in an adaptive fashion: Given a nominal point $\mathbf{x} \in X$ and a perturbed point $\mathbf{x}'$, we run the stochastic simulation algorithm an initial number of times N, independently for each. From the resulting collection of output traces, we extract the corresponding observable values $\{y_1, \ldots, y_N\}$ for $\mathbf{x}$ and $\{y_1', \ldots, y_N'\}$ for $\mathbf{x}'$. We then continue to do further repetitions of the simulations until one of two stopping criteria is met: either i) the runtime limit is reached, or ii) we have achieved a desired *angle of gradient uncertainty* (to be defined below). In both cases, the averages of the collections $\{y_i\}_{i \in \mathbb{N}}$, $\{y_i'\}_{i \in \mathbb{N}}$ are returned along with other parameters of interest.

In the following subsections, we give the remaining details. A graphical representation of the workflow for a single nominal point is given in Figure 1.
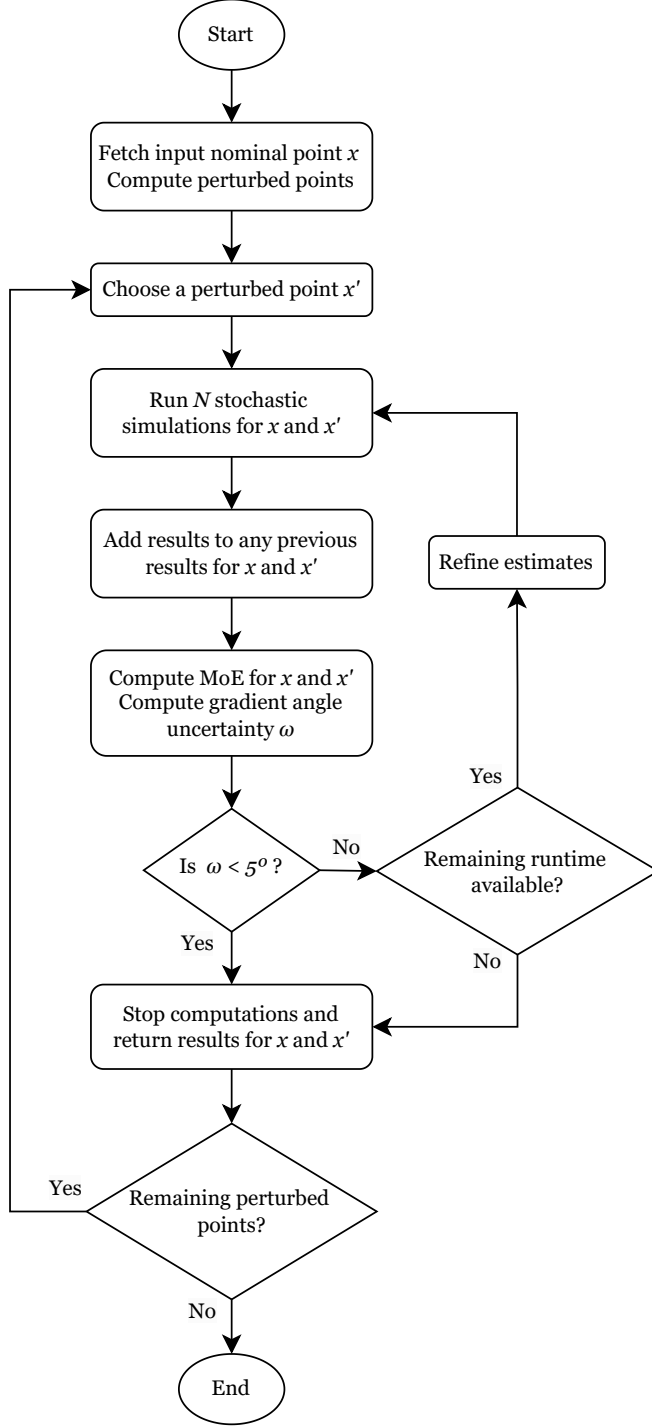
Figure 1: Data Collection Workflow. For each nominal–perturbation pair, we first run a batch of N simulations, evaluate the gradient uncertainty angle ω (see Figure 2), and, if necessary, refine the estimates by running additional batches of N simulations for both points. Because the stopping criterion depends on the pair, the same number of extra simulations is assigned to each point. This strategy could be further optimized by: i) distributing extra simulations according to each point's individual uncertainty, and ii) reusing nominal-point simulations for multiple perturbation points.

4.2 Gradient Approximation

Since we are considering stochastic systems—with internal noise and fluctuations—we, as outlined above, are interested in the sensitivity of the expected value of the model observable, $\mathbb{E}[f(\mathbf{x})] = \bar{f}(\mathbf{x}) = \bar{y}$ to perturbations in nominal points $\mathbf{x} \in X$. Since we are only interested in the observable at a single simulation time point, we omit time from the notation. We characterize the sensitivity via the estimation of the gradient vectors

$$\nabla \bar{f}(\mathbf{x}) = \left[\frac{\partial \bar{f}}{\partial x_1}(\mathbf{x}), \ldots, \frac{\partial \bar{f}}{\partial x_n}(\mathbf{x}) \right].$$

The partial derivatives can be scaled in order to make them independent of the units of f and x_j [29, 32]. To approximate the gradient vector, we employ a finite difference approximation, specifically using forward differences [36, 8, 16]. While we acknowledge the variety of methodologies available for gradient estimation, this study focuses on presenting the general framework rather than exploring specific techniques. We consider the forward differences method to be appropriate for its computational simplicity and ease of interpretation [29].

Given $\mathbf{x} = (x_1, \ldots, x_n) \in X$, we calculate perturbation vectors by incrementing each dimension by a small amount $h > 0$. Specifically, for dimension $j \in \{1, \ldots, n\}$, we consider the perturbed point $\mathbf{x}'_j = (x_1, \ldots, x_j + h, \ldots, x_n)$. As h approaches zero, the forward difference

$$Z_{\mathbf{x},j} = \frac{\bar{f}(\mathbf{x}'_j) - \bar{f}(\mathbf{x})}{h}$$

tends towards the partial derivative $\frac{\partial \bar{f}}{\partial x_j}(\mathbf{x})$ evaluated at $h = 0$. However, in stochastic systems, h needs to be balanced: it should be small enough to reduce the truncation error in the forward difference approximation, which is caused by ignoring higher-order terms in a Taylor series approximation, but large enough to avoid simulation-related errors, such as rounding errors or noise in the stochastic simulations [18]. The approximated gradient vector is given by

$$\nabla \bar{f}(\mathbf{x}) \approx \left(\frac{\bar{f}(\mathbf{x}'_1) - \bar{f}(\mathbf{x})}{h}, \ldots, \frac{\bar{f}(\mathbf{x}'_n) - \bar{f}(\mathbf{x})}{h} \right) = (Z_{\mathbf{x},1}, \ldots, Z_{\mathbf{x},n}).$$

The resulting gradients can be graphically represented in a vector field, thereby visualizing the model's sensitivity to changes in the input parameters across the parameter space X.

4.3 Simulation Stopping Criterion: Gradient Range of Angle Uncertainty

Given $\mathbf{x} \in X$, the model observable $f(\mathbf{x})$ is a stochastic variable where the uncertainty is linked to the internal stochastic effects within the system. The variable distribution, population mean $\mathbb{E}[f(\mathbf{x})] = \bar{f}(\mathbf{x})$, and population standard deviation σ are unknown. To approximate $\bar{f}(\mathbf{x})$ we need to run simulations a sufficient number of times. As a key component of our methodology, this sample size will be dynamically adjusted based on the uncertainty present in the gradient approximation. Then the mean of the final sample is used as the estimate of $\bar{f}(\mathbf{x})$. We will break this down in the following.

To obtain a reliable gradient approximation, our approach is to minimize the uncertainty in the slopes $Z_{\mathbf{x},1}, \ldots, Z_{\mathbf{x},n}$. For a slope $Z_{\mathbf{x},j}$ this uncertainty can be regarded as an *angle* that represents the range inside which many possible slopes can exist—each potentially being the one connecting the true population means of $f(\mathbf{x})$ and $f(\mathbf{x}'_{\mathbf{j}})$. When running N initial simulations to obtain $f(\mathbf{x})$ and $f(\mathbf{x}'_{\mathbf{j}})$, we can calculate the 95 % confidence intervals (CI) for $\bar{f}(\mathbf{x})$ and $\bar{f}(\mathbf{x}'_{\mathbf{j}})$. Recall that
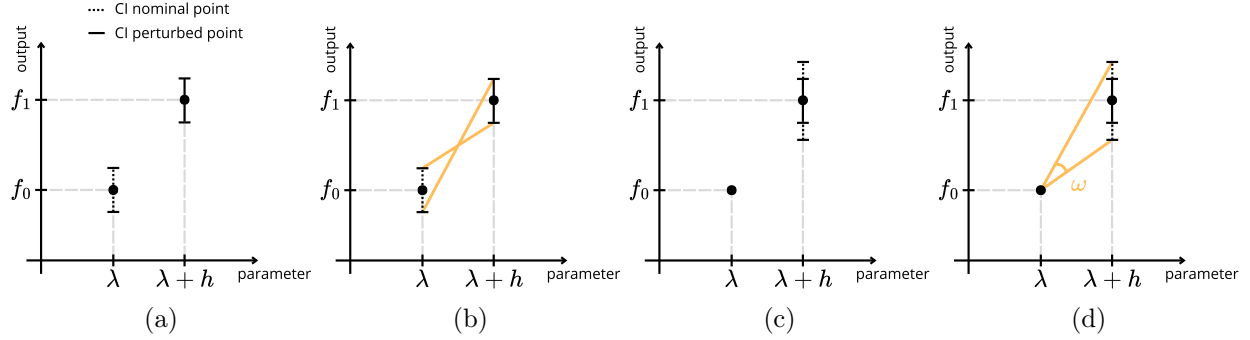
Figure 2: Angular range of gradient uncertainty ω. a The individual confidence intervals (CIs) for both the nominal point and its perturbation in one dimension. b The extreme possible gradients. c Combination of the confidence intervals to simplify the range of uncertainty. d The angular range within which the possible gradients exist.

the characteristics of CIs is that with 95 % confidence, the true population mean lies somewhere within it (given suitable assumptions on the probability distribution in question). In other words, the interval defines a range of plausible values for the true mean, based on the observed data. Therefore, the width of the interval, determined by the margin of error (MoE), represents the scope within which the gradient likely lies. This scope can be characterized by an angle ω—the range of gradient uncertainty. Figure 2 illustrates ω. As the number of simulations increases to $2N, 3N, \ldots$ (see Figure 1), the confidence interval narrows, resulting in a decrease in the uncertainty angle ω. This angle is a way to quantify and control the confidence in the gradient estimation and hence of the outcome of the sensitivity analysis. In this paper, we set as our goal to run simulations to achieve $\omega < 5°$ before timeout (but other angle uncertainty thresholds could be chosen, of course).

This approach, where we dynamically adjust the sample size based on the observed variability, not only gives control over the the precision of the analysis, but also ensures that just enough data is collected per point to achieve the desired precision, avoiding unnecessary sampling and saving time and resources.

4.4 Computing Confidence Intervals

Our approach relies on statistical principles to ensure reliability in our estimates. Given a sample $\{y_1, \ldots, y_N\}$, by the Law of Large Numbers, the sample mean $\bar{y} = \frac{\sum_{i=1}^{N} y_i}{N}$ is an unbiased estimator of the true population mean μ, i.e., as N increases, $\bar{y}$ converges to μ. By the Central Limit Theorem, for N large enough the distribution of the sample mean $\bar{y}$ approximates the normal distribution with mean μ and standard deviation $\sigma/\sqrt{N}$, regardless of the shape of the original distribution (assuming finite variance) [7, 31, 20]. This implies that we can quantify the uncertainty in the estimate $\bar{y}$ using confidence intervals.

Every time we run a new batch of simulations for a parameter vector $\mathbf{x}$ (nominal or perturbed), we compute the sample mean $\bar{y}$ and sample standard deviation S, given by

$$S = \sqrt{\frac{\sum_{i=1}^{N}(y_i - \bar{y})^2}{N - 1}}.$$

For a confidence level α, we then determine the two-sided t-value $t_{N-1,\alpha/2}$ corresponding $N - 1$

degrees of freedom. The margin of error is then:

$$\text{MoE} = t_{N-1,\alpha/2} \frac{S}{\sqrt{N}}.$$

The confidence interval for the sample mean is then defined as:

$$CI = \left[\bar{y} - \text{MoE}, \ \bar{y} + \text{MoE} \right].$$

This interval informs of the precision of the estimate $\bar{y}$ for the true mean μ. Wider intervals indicate more uncertainty due to great variability in our data or smaller sample sizes. Therefore, the confidence interval serves as a way to interpret the reliability of simulation outcomes.

4.5   Global Sensitivity Coefficients

To better understand the relative impact of each input variable on the expected model observable $\bar{f}(\mathbf{x})$, we may be interested in calculating an overall numerical sensitivity coefficient for each input variable. For this purpose, given the approximated gradient vector $\nabla \bar{f}(\mathbf{x})$ at $\mathbf{x} \in X'$, we extract the absolute value of each component:

$$\left| Z_{\mathbf{x},1} \right|, \ldots, \left| Z_{\mathbf{x},n} \right|.$$

We define the sensitivity coefficient for the jth input variable x_j, $j \in \{1, \ldots, n\}$, as the average of these absolute values across all sampled points [29]:

$$SC_j = \frac{1}{M} \sum_{i=1}^{M} \left| Z_{\mathbf{x}^i,j} \right|,$$

where M denotes the total number of sampled points.

This measure represents the average absolute rate of change of $\bar{f}(\mathbf{x})$ with respect to the jth variable. It is intended to provide a quantitative assessment of the observable's sensitivity to a given variable based on the approximated gradients.

5   Application Examples

In this section we will show applications of our methodology. The approach itself is general and can be applied in many domains—we here choose chemical systems as an illustrative setting in which reaction rate constants constitute a natural choice of parameters to perform sensitivity analysis on. We use the cheminformatics software MØD [2] as our vehicle for modeling the systems in a rule-based fashion—in particular, we use MØD's stochastic simulation module [21] for performing Gillespie-based stochastic simulations. In rule-based modeling, a single rule represents several reactions with the same mechanism, hence systems can often be modeled by a small number of reaction rules. Assigning reaction rate constants to rules rather than individual reactions thus helps keeping the number of parameters in the sensitivity analysis down. In all our experiments, the input parameters will be the reaction rate constants for the rules of the system, while custom observable measures will be defined for each system.

We will be working with three-dimensional parameter spaces $X \subseteq \mathbb{R}^3_{\geq 0}$. In particular, we consider points $\mathbf{x} = (x_1, x_2, x_3)$ in the 2-simplex
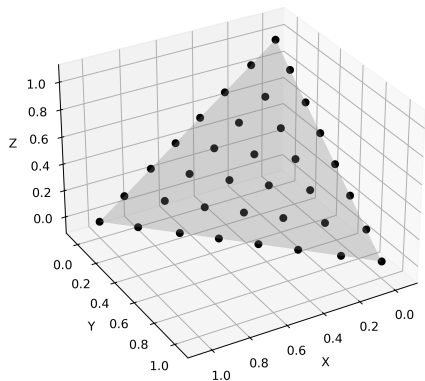
Figure 3: Input parameter points in the 2-simplex.

$$\mathbf{x} \in \left\{ (x_1, x_2, x_3) \in \mathbb{R}^3 \;\middle|\; \sum_{i=1}^{3} x_i = 1, \; x_i \geq 0 \right\},$$

as illustrated in Figure 3. Scaling all reaction rates by a common factor only changes the speed at which the chemical system evolves, not the (probability distribution of the) outcome of the simulation. Therefore, we normalize the rates such that their sum is a constant, here chosen to be one.

We present the main results of the sensitivity analysis as a series of 2D plots. Our data (points on the simplex and their estimated gradient vector) are of course 3D objects, but such data is notoriously hard to present in a clearly readable fashion, hence this choice of presentation. To help the interpretation, we show the points and their gradients in two different types of projections: a projection onto the plane of the simplex and three projections onto the three basic 2D planes of the 3D coordinate system (as an example, see Figure 5 below). In the latter type of projections, the two axes represent the rate constants of two of the three reactions (the remaining rate constant is given by the requirement that the three rates sum to one). The vectors shown are the gradient at each point, subjected to the same projection and colored to show the value of the observable at the point in question. To improve readability, the vectors have been scaled so that the maximum length appearing equals the distance between points.

We consider two concepts that will help analyze our results—both encapsulating a notion of robustness, but in different ways. One concept is *local sensitivity*, which refers to how much the average value of the observable changes in response to small perturbations of the input parameters in a given region of the input space. A region is considered robust in this sense (low local sensitivity) if such perturbations lead to relatively minor changes in the observable values. Another concept is *gradient reliability*, which refers to the consistency of gradient estimates in light of the stochastic nature of the simulations. A result is considered reliable if repeated simulations under the same conditions yield similar outcomes, represented in our case by smaller confidence intervals (or equivalently, a smaller range of angle uncertainty). See Figure 2d.

As will be shown in the examples, we can encounter situations where the observable displays little relative change to perturbations of the input parameters (low local sensitivity), but where the uncertainty intervals for gradients are large due to internal stochastic noise (low gradient reliability). The other way around, a gradient might be produced by consistent estimates (high reliability), even if small perturbations cause large observable changes (high local sensitivity). In fact, all four combinations of sensitivity and reliability are possible.
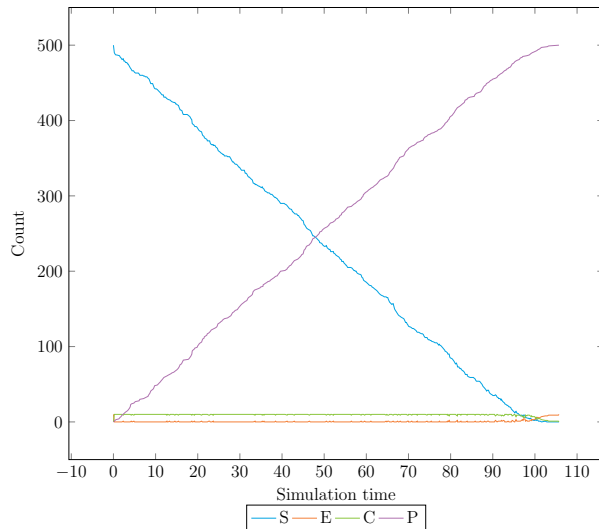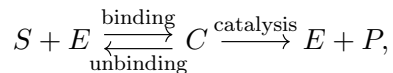
12

Figure 4: Stochastic simulation of the evolution (simulation time units) of Michaelis-Menten dynamics.

5.1 Michaelis-Menten Kinetics

The Michaelis-Menten kinetics [33, 22] model general enzyme catalysis. Here, we consider the simplified reaction scheme, consisting of the reactions

$$S + E \; \underset{\text{unbinding}}{\overset{\text{binding}}{\rightleftharpoons}} \; C \xrightarrow{\text{catalysis}} E + P,$$

where S represents the substrate, E is the enzyme, C is the complex resulting from binding the substrate to the enzyme, and P is the product.

We apply the sensitivity analysis procedure described above and consider the reaction rate constant of each of the three reactions as the input parameters. For observable, we choose the simulation time (by which we mean units of time in the simulated process) until all substrate S is consumed. The initial molecular counts are 500 units of substrate S and 10 units of enzyme E. As an illustrative example, one simulation of the evolution of the Michaelis-Menten dynamics using the stochastic simulation module in MØD produces the output in Figure 4 when all rate constants are 0.5. For the sensitivity analysis we used the following setup.

- Initial number of simulations N per input point $\mathbf{x} \in X$: 50.

- Runtime limit for simulating each $\mathbf{x} \in X$: 300 seconds wall clock time.

- Confidence level for margin of error calculation: $\alpha = 0.95$.

- Target angle of gradient uncertainty: $\omega = 5°$.

- Size of the perturbation (h) for gradient estimation: 50 % of the distance between input points.

Figure 5 depicts our results. These show that the system is most sensitive to changes in the catalysis rate constant, especially for values of it close to zero (but non-zero), as this is where vector magnitudes are largest. In contrast, variations in binding and unbinding rate constants lead to little change in the observable, indicating low relative sensitivity. Points marked by a cross indicate that

13

(a) Projected gradient vectors.

(b) 3D magnitude colour map.

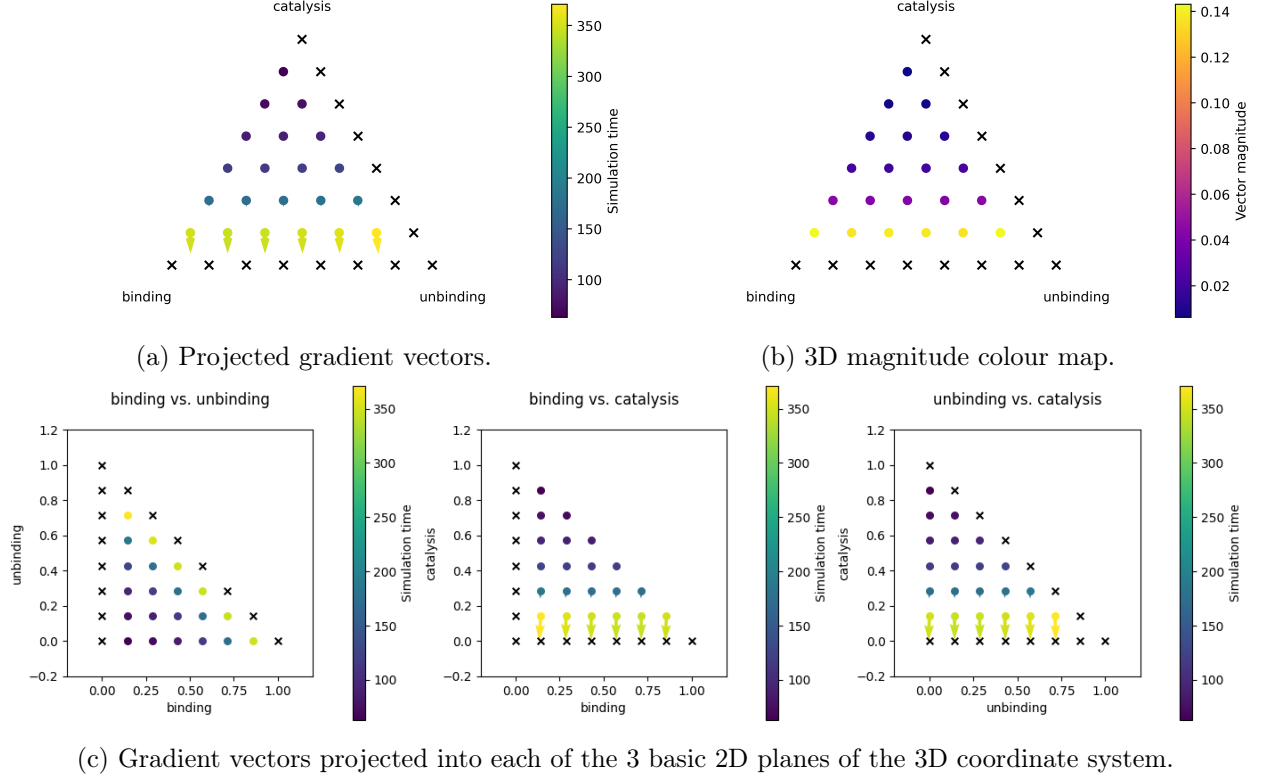(c) Gradient vectors projected into each of the 3 basic 2D planes of the 3D coordinate system.

Figure 5: Sensitivity analysis of the Michaelis-Menten Kinetics. a The 2-simplex with the gradient vectors projected into the simplex plane. The points and vectors are colored according to the value of the observable (simulation time to consume S). b The 2-simplex with each sampled point colored according to the magnitude of the full non-projected gradient vector. c Gradient vectors projected onto the three basic 2D planes of the 3D coordinate system. The points and vectors are colored according to the value of the observable (simulation time to consume S). From the plots we observe that as the rate constant for catalysis increases, the simulation time to consume S decreases. The gradient vectors exhibit their largest magnitude when the catalysis rate constant is close to zero, indicating that in this area of the parameter space, the sensitivity is highest. The direction of the gradient shows that the sensitivity is largest with respect to the catalysis rate constant.

no observable was produced during the simulation: these are the points where either the binding or the catalysis reactions had a rate constant of zero, which prevents the substrate S from being depleted. Overall, the analysis shows that the catalysis rate constant is the key driver of variation of this observable (the simulation time until S is fully consumed), and that there are clear parameter regions, aligned with the magnitude of the catalysis rate constant, that minimize or maximize the value of the observable.

The catalysis dimension shows the highest sensitivity in Figure 5c, while yielding the most stable gradient estimates, as reflected by its low average angle uncertainty in Table 2. In contrast, the binding and unbinding dimensions show low sensitivity but high angle of uncertainty. This is likely due to the fact that the observable changes very little in response to variations in those axes, making gradient estimates more susceptible to noise.

In order to calculate the global sensitivity coefficients described in section Global Sensitivity Coefficients, we repeat the full experiment described in the bullet points above five times and collect the data in Table 3. This data summarizes the effect we observe in Figure 5, highlighting

	Mean	Min	Max	Std Dev
Angle of Gradient Uncertainty	15.681	0.029	76.957	19.574

Table 1: Summary statistics for the angle of gradient uncertainty, measured in degrees. Values show considerable variation across the input space.

Dimension	Avg Angle Uncertainty
Binding	20.905
Unbinding	25.364
Catalysis	0.774

Table 2: Average angle of gradient uncertainty grouped by dimension. The low value for catalysis indicates greater stability in the estimated gradient direction along that parameter.

the strong relative sensitivity of the observable measure to the catalytic rate constant. We observe that the sensitivity coefficients show little variation across experiments, as indicated by their small standard deviation.

Our initial objective was to reduce the angle of gradient uncertainty to at most $5°$, as a criterion for the number of simulations required. However, the summary statistics in Table 1 show that in the available time, we achieved an average angle of approximately $15.7°$, with a substantial standard deviation of $19.6°$ and a wide range from $0.03°$ to $77°$. This spread highlights significant variability in gradient estimation accuracy across the parameter space, in other words, some regions provide more stable directions than others. This information can be used to run further additional simulations in the noisiest regions in order to improve accuracy.

Figure 6 extends the above statistics on angles by plotting the number of times (in percent across all nominal points and perturbation experiments) that we achieved a given angle bound when we conducted the experiments with different runtime limits. For example, for a runtime limit of 300 seconds wall clock time per nominal point and perturbation pair, about $45\,\%$ of the nominal-perturbation pairs achieved an angle smaller than $5°$, while $63\,\%$ achieved an angle smaller than $15°$. For a runtime limit of 1200 seconds, $60\,\%$ of the nominal point and perturbation pairs achieved an angle smaller than $5°$. One noticeable difference is in the maximum angle obtained for each time limit, ranging approximately from $35°$ (purple) to $145°$ (blue). In larger percentiles, we can observe more potential for better angle ranges when allowing longer runtime limits.

5.2 Formose Chemistry

We consider a simplified, rule-based model of the formose chemistry following Andersen et al. [1]. Starting from formaldehyde and glycolaldehyde, a small set of reaction rules—aldol addition (for-

Dimension	Mean	Min	Max	Std Dev
Binding	42.809	37.436	45.596	3.195
Unbinding	17.296	16.441	17.876	0.721
Catalysis	866.765	857.019	874.932	6.695

Table 3: Statistics for the global sensitivity coefficient for each input parameter.
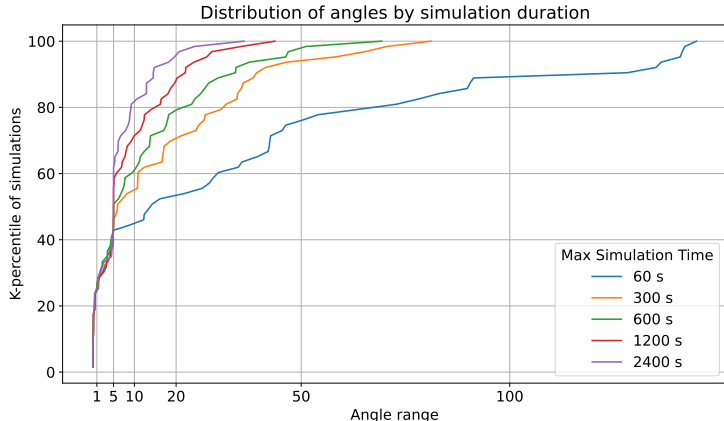
Figure 6: Percentile distribution of the number of times a given angle bound was reached, across all nominal points and perturbations. Each colored line corresponds to a different runtime limit used when simulating each nominal–perturbation pair.

ward/backward) and keto–enol tautomerization—generates the reaction network on-the-fly. We simulate the dynamics using Gillespie's stochastic simulation algorithm as implemented in MØD. Our objective here is to analyze how the diversity of the chemical space depends on these reaction-type rate constants.

The details of the experiment are as follows. Consistent with our motivation to keep the parameter space tractable, we assign rate parameters based on reaction types. Thus, the input parameters are the rate constants of the reaction rules depicted in Figure 7. We also equate the rate constants of the two keto-enol rules (forward and backward) such that these constitute a single input parameter. The observable, aimed at measuring the diversity of the chemical space, is the total number of different molecular species created throughout the simulation after a fixed simulation time. The initial state is composed of 500 copies of formaldehyde and 50 copies of glycolaldehyde. To limit the combinatorial explosion of compounds, the molecular size is capped at eight carbon atoms. Additionally, unlike in the previous example, here we utilize a simulation time limit parameter in MØD for each simulation instance. Further experimental design choices are:

- Initial number of simulations N per input point $\mathbf{x} \in X$: 50.

- Runtime limit for simulating each $\mathbf{x} \in X$: 300 seconds wall clock time.

- Simulation time limit of individual simulation instances: 20 simulation time units.

- Confidence level for margin of error calculation: $\alpha = 0.95$.

- Target angle of gradient uncertainty: $\omega = 5°$.

- Size of the perturbation (h) for gradient estimation: 50 % the distance between input points.

We note that in systems like the formose chemistry, ODE modeling would not be suitable for conducting this experiment since the reaction network is not known in advance. Here, we begin only with a set of initial compounds and a few reaction rules, and the chemical space is then expanded on-the-fly by MØD. In this context, sensitivity analysis must rely on averaging multiple simulation realizations, given that each run may explore different reaction paths. This stochastic approach allows us to estimate the system's overall response to changes in input parameters, without requiring
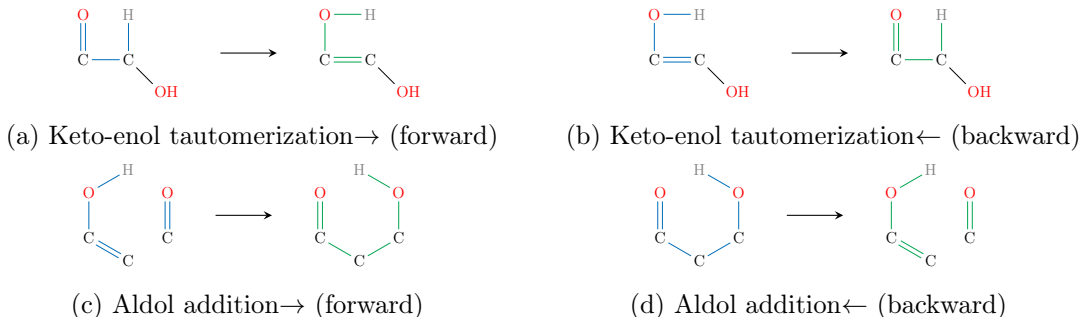
(a) Keto-enol tautomerization→ (forward) (b) Keto-enol tautomerization← (backward)

(c) Aldol addition→ (forward) (d) Aldol addition← (backward)

Figure 7: Reaction rules for the formose chemistry model.

	Mean	Min	Max	Std Dev
Angle Uncertainty	20.604	0.000	118.630	35.463

Table 4: Summary statistics for the angle of gradient uncertainty, measured in degrees. High variation across the input space can be seen.

a complete, static reaction network—which in the case of formose chemistry can be of substantial size—available beforehand.

The results of the experiment are illustrated in Figure 8. We can observe that the system is most sensitive to changes along the aldol-addition→ axis around the area where this parameter is zero. This indicates that going from no activity to a little bit increases dramatically the diversity of species in the chemical space (seen by the abrupt change from purple to yellow points). The relatively high sensitivity of the observable to changes along this axis in this specific region of the space creates the visual effect that changes in other axes, or in other regions, do not have an impact on the system. This is partly because, for legibility reasons, we scale vectors such that the largest vector in the plot has a length equal to the distance between neighboring nominal points. We can, however, appreciate a slight sensitivity with respect to changes along the keto-enol axis in the area where this parameter is zero.

To investigate further the remaining areas, we remove points with zeroes in their coordinates (and rescale the remaining vectors), by which we obtain Figure 9. Here, the sensitivity of the system (length of vectors) displays a different pattern: the system seems sensitive to changes in reaction rate constants for both the aldol-addition← and keto-enol rules, but especially for the keto-enol rules, in the region of space where this parameter takes values closer to zero. An interesting maximal point (yellow) can be observed, where the chemical space is as diverse as it can get in the chosen amount of simulation time. Lower diversity is in general achieved for low rate constants along the keto-enol axis, as indicated by the darker purple points.

Table 4 presents a summary of the angles of gradient uncertainty obtained for this experiment. Here, we observe an average angle uncertainty of around 20.6°. A high standard deviation indicates a non-uniform achieved accuracy for the gradient estimates, which are highly dependent on the region of space and the dimension being perturbed.

From Figure 8, we learned that the observable is most sensitive to changes along the aldol-addition→ axis, showing relatively lower sensitivity to changes in the other two parameters. Table 5 further suggests that the aldol-addition→ rule not only contributes the most to the system's sensitivity, but also has the highest estimate uncertainty, by a considerable margin. In contrast, the remaining dimensions yield relatively stable gradient estimates.

(a) Projected gradient vectors.

(b) 3D magnitude colour map.

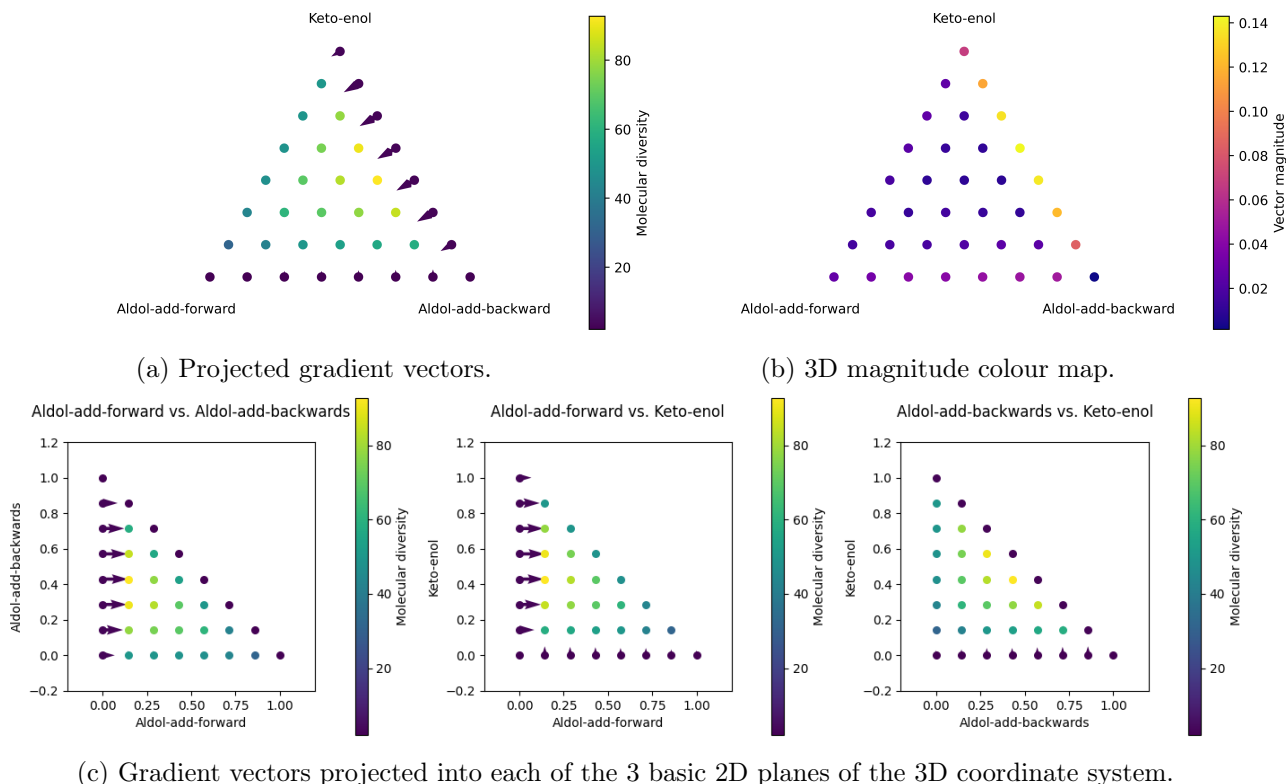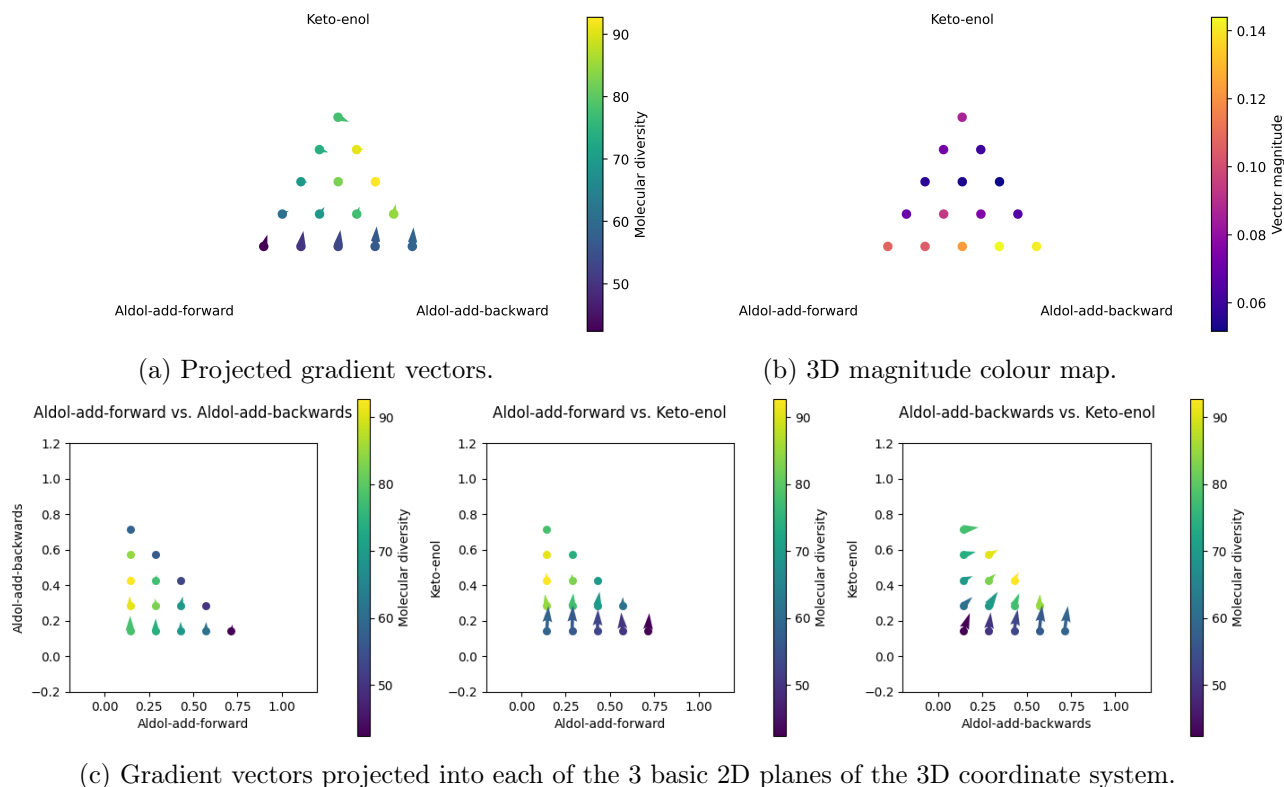(c) Gradient vectors projected into each of the 3 basic 2D planes of the 3D coordinate system.

Figure 8: Sensitivity analysis of the formose model. a The 2-simplex with the gradient vectors projected into the simplex plane. The points and vectors are colored according to the value of the observable (number of different molecular species created throughout the simulation). b The 2-simplex with each sampled point colored according to the magnitude of the full non-projected gradient vector. c Gradient vectors projected onto the three basic 2D planes of the 3D coordinate system. The points and vectors are colored according to the value of the observable. These plots indicate that the observable, the number of different molecular species created throughout the simulation, is more sensitive to changes along the aldol-addition$\rightarrow$ axis. The highest sensitivity is achieved in the region where this parameter equals zero.

Dimension	Avg Angle Uncertainty
Aldol-add-forward	50.167
Aldol-add-backward	2.736
Keto-enol	8.910

Table 5: Average angle of gradient uncertainty grouped by dimension. A high value for the aldol-addition$\rightarrow$ rule rate constant indicates a significantly lower accuracy in gradient estimates when moving along this axis, compared to the other two input parameters.

(a) Projected gradient vectors.

(b) 3D magnitude colour map.

(c) Gradient vectors projected into each of the 3 basic 2D planes of the 3D coordinate system.

Figure 9: Sensitivity analysis of the formose model. a The 2-simplex with the gradient vectors projected into the simplex plane. The points and vectors are colored according to the value of the observable (number of different molecular species created throughout the simulation). b The 2-simplex with each sampled point colored according to the magnitude of the full non-projected gradient vector. c Gradient vectors projected onto the three basic 2D planes of the 3D coordinate system. The points and vectors are colored according to the value of the observable. In this new set of plots we have removed points with zero coordinates. In this setup, the observable is more sensitive to changes along the keto-enol axis, and to changes in the aldol-addition→ rate constant in second place. Highest sensitivity is achieved in the region where the keto-enol rate constants are small.

Dimension	Mean	Median	Min	Max	Std Dev
Aldol-add-forward	220.722	220.8	219.664	221.538	0.714
Aldol-add-backward	59.136	58.76	57.12	61.196	1.526
Keto-enol	127.676	127.615	125.139	129.763	1.728

Table 6: Statistics for the global sensitivity coefficient for each parameter.
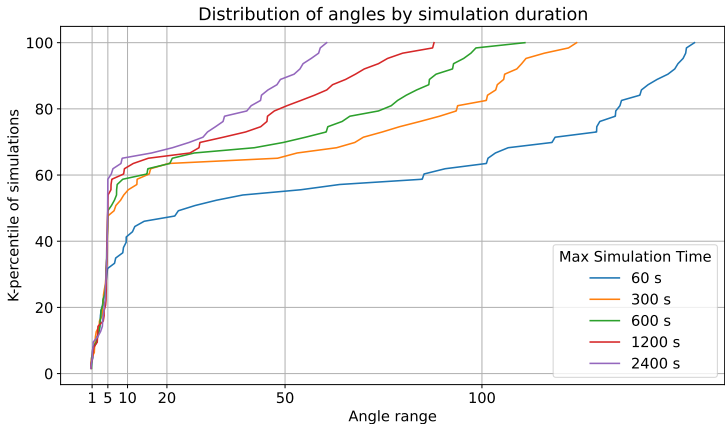

Figure 10: Percentile distribution of the number of times each indicated angle range was reached, across all nominal points and perturbations. Each colored line corresponds to a different runtime limit used when simulating each nominal–perturbation pair.

We repeat the experiment five times to generate statistics on the global sensitivity coefficients. Table 6 provides a summary. As the concluding remark, the aldol-addition→ rate constants impact the system's diversity the most, followed by both keto-enol rule rate constants.

In Figure 10, we extend the statistics of Table 4 on angles by plotting the number of times (in percent across all nominal points and perturbation experiments) that we achieved a given angle bound when we conducted the experiments with different runtime limits. It can be observed that, in approximately 50 % of the cases, we reached the 5° angle bound when the time limit is equal to or greater than 300 seconds wall clock time. When we increase the available simulation time, we observe a moderate increase in the percentage of cases where we obtained a bound of 5° or less, ranging from approximately 35 % (blue) to 60 % (purple). Similarly to the example above, the maximum angle obtained for each time limit varies widely, ranging approximately from 60° (purple) to 153° (blue).

5.3 Further Examples of Observables

Note that a strong aspect of our methodology is the flexibility to work with many different observables. The possibilities are wide: as previously mentioned, in MØD we can retrieve the simulation trace of events, where each rule application (and chemical reaction instantiated by this rule) is specified. *Dynamic* information, such as event times, molecular species at each simulation step, and species counts over time, is accessible. From this, one can define dynamic observables such as the time until a certain molecule appears or until the first application of a specific rule (more generally, the time to an event of interest), the distribution of molecular counts over time, or the total distribution of rule applications. Additionally, *structural* information is also available, including

molecular structures down to the atomic level, which allows for defining observables such as identifying structural motifs, finding specific molecules, or simply counting atoms like carbons. Chemical network properties, such as the size of the network, like in our formose example, are also available. Taken together, this combination of dynamic and structural information supports the construction of a broad and flexible set of observables.

As concrete examples, for the formose system in subsection Formose Chemistry we experimented with the following additional observables:

- Count of pentoses: we created a function that analyzes the chemical structure of each species, checks whether it is a carbohydrate, and counts the number of carbons. We can analyze variations in pentose count throughout the simulation, or focus on the amount obtained at the final simulation time.

- Count of a specific molecular pattern: for example, structures with branched carbons or formose-related chemical motifs. We used MØD's monomorphism check to search for specific substructures in our chemical space. Concretely, the following SMILES patterns: `[C][C]([C])([C])`, and `OCC(O)C(O)C=O`.

- Count of specific molecules: we analyzed the sensitivity to changes in the counts of both glycolaldehyde and formaldehyde at the end of the simulation.

The sensitivity analysis conclusions were essentially the same as those already reported in Formose Chemistry, hence, for reasons of space, we omit plots for those additional experiments.

5.4 Technical Details

Computations were performed on a laptop with a 13th Gen Intel Core i7-13700H processor with 32 GB of RAM, using Python 3.10 and MØD version 0.16.1.77. Note that the methodology allows for a high degree of parallelism; here, we parallelized the simulations conducted for the nominal point and the perturbation point. The total runtime for conducting one experiment of the Michaelis-Menten system, allowing a runtime limit of 300 seconds per simulated nominal–perturbation, and evaluating 84 input points (nominal and perturbed), took 2 hours and 56 minutes. For the formose system, for the same runtime limit and the same number of points, 3 hours and 19 minutes.

6 Conclusion

In the context of stochastic chemical systems, many global techniques demand extensive simulation runs to reduce noise-related uncertainty. This can become computationally prohibitive if each simulation is expensive or if the parameter space must be densely sampled to capture interactions. Because rule-based models often have a relatively small set of core parameters (even if they generate a combinatorially large network of species on-the-fly), a local gradient-based approach across multiple parameter points can be both feasible and illuminating. By adaptively increasing simulation replicates until reaching a desired level of gradient uncertainty, the randomness from stochastic runs is systematically controlled. In addition, limiting the analysis to a small parameter set simplifies result visualization and keeps computational demands within reason. Thus, the proposed method retains the simplicity of local, derivative-based analysis while offering a moderately global perspective by sampling parameter space more broadly—especially suitable for rule-based and combinatorially complex chemical systems. This synergy allows for straightforward "black-box" repeated simulations, customized observables, and effective exploration of the sensitivity across the parameter space, yielding practical insights into model robustness and parameter importance.

Acknowledgement

References

[1] Jakob L Andersen, Christoph Flamm, Daniel Merkle, and Peter F Stadler. Generic strategies for chemical space exploration. *International journal of computational biology and drug design*, 7(2-3):225–258, 2014.

[2] Jakob L Andersen, Christoph Flamm, Daniel Merkle, and Peter F Stadler. A software package for chemically inspired graph transformation. In *Graph Transformation: 9th International Conference, ICGT 2016, in Memory of Hartmut Ehrig, Held as Part of STAF 2016, Vienna, Austria, July 5-6, 2016, Proceedings 9*, pages 73–88. Springer, 2016.

[3] David F Anderson. An efficient finite difference method for parameter sensitivities of continuous time markov chains. *SIAM Journal on Numerical Analysis*, 50(5):2237–2258, 2012.

[4] RW Atherton, RB Schainker, and ER Ducot. On the statistical sensitivity analysis of models for chemical kinetics. *AIChE Journal*, 21(3):441–448, 1975.

[5] Anthony F Bartholomay. Stochastic models for chemical reactions: I. theory of the unimolecular reaction process. *The bulletin of mathematical biophysics*, 20:175–190, 1958.

[6] Gil Benkö, Christoph Flamm, and Peter F Stadler. A graph-based toy model of chemistry. *Journal of Chemical Information and Computer Sciences*, 43(4):1085–1093, 2003.

[7] Dimitri Bertsekas and John N Tsitsiklis. *Introduction to probability*, volume 1. Athena Scientific, 2008.

[8] Richard L. Burden and J. D. Faires. *Numerical analysis*. Brooks/Cole, Pacific Grove, CA, 7th edition, 2001.

[9] Lily A Chylek, Leonard A Harris, Chang-Shung Tung, James R Faeder, Carlos F Lopez, and William S Hlavacek. Rule-based modeling: a computational approach for studying biomolecular site dynamics in cell signaling systems. *Wiley Interdisciplinary Reviews: Systems Biology and Medicine*, 6(1):13–36, 2014.

[10] Vicente Costanza and John H Seinfeld. Stochastic sensitivity analysis in chemical kinetics. *The Journal of chemical physics*, 74(7):3852–3858, 1981.

[11] RI Cukier, HB Levine, and KE Shuler. Nonlinear sensitivity analysis of multiparameter model systems. *Journal of computational physics*, 26(1):1–42, 1978.

[12] RI Cukier, JH Schaibly, and Kurt E Shuler. Study of the sensitivity of coupled reaction systems to uncertainties in rate coefficients. iii. analysis of the approximations. *The Journal of Chemical Physics*, 63(3):1140–1149, 1975.

[13] Chiara Damiani, Alessandro Filisetti, Alex Graudenzi, and Paola Lecca. Parameter sensitivity analysis of stochastic models: Application to catalytic reaction networks. *Computational biology and chemistry*, 42:5–17, 2013.

[14] Vincent Danos, Jérôme Feret, Walter Fontana, Russell Harmer, and Jean Krivine. Rule-based modelling of cellular signalling. In *International conference on concurrency theory*, pages 17–41. Springer, 2007.

[15] Andrea Degasperi and Stephen Gilmore. Sensitivity analysis of stochastic models of bistable biochemical reactions. In *International School on Formal Methods for the Design of Computer, Communication and Software Systems*, pages 1–20. Springer, 2008.

[16] Michael C Fu. *Stochastic gradient estimation.* Springer, 2015.

[17] Daniel T Gillespie. A general method for numerically simulating the stochastic time evolution of coupled chemical reactions. *Journal of computational physics*, 22(4):403–434, 1976.

[18] Rudiyanto Gunawan, Yang Cao, Linda Petzold, and Francis J Doyle. Sensitivity analysis of discrete stochastic systems. *Biophysical journal*, 88(4):2530–2540, 2005.

[19] Michał Komorowski, Maria J Costa, David A Rand, and Michael PH Stumpf. Sensitivity, robustness, and identifiability in stochastic chemical kinetics models. *Proceedings of the National Academy of Sciences*, 108(21):8645–8650, 2011.

[20] Sang Gyu Kwak and Jong Hae Kim. Central limit theorem: the cornerstone of modern statistics. *Korean journal of anesthesiology*, 70(2):144–156, 2017.

[21] Erika M. Herrera Machado, Jakob L. Andersen, Rolf Fagerberg, Christoph Flamm, Daniel Merkle, and Peter F. Stadler. Rule-based gillespie simulation of chemical systems, 2025.

[22] Leonor Michaelis and Maude L Menten. The kinetics of the inversion effect. *Biochem. Z*, 49:333–369, 1913.

[23] David Miller and Michael Frenklach. Sensitivity analysis and parameter estimation in dynamic modeling of chemical kinetics. *International Journal of Chemical Kinetics*, 15(7):677–696, 1983.

[24] Jérôme Morio. Global and local sensitivity analysis methods for a physical system. *European journal of physics*, 32(6):1577, 2011.

[25] Max D Morris. Factorial sampling plans for preliminary computational experiments. *Technometrics*, 33(2):161–174, 1991.

[26] Monjur Morshed, Brian Ingalls, and Silvana Ilie. An efficient finite-difference strategy for sensitivity analysis of stochastic models of biochemical systems. *Biosystems*, 151:43–52, 2017.

[27] Jorge Nocedal and Stephen J Wright. *Numerical optimization.* Springer, 1999.

[28] Sergey Plyasunov and Adam P Arkin. Efficient stochastic sensitivity analysis of discrete event systems. *Journal of Computational Physics*, 221(2):724–738, 2007.

[29] Herschel Rabitz, Mark Kramer, and D Dacol. Sensitivity analysis in chemical kinetics. *Annual review of physical chemistry*, 34(1):419–461, 1983.

[30] Muruhan Rathinam, Patrick W Sheppard, and Mustafa Khammash. Efficient computation of parameter sensitivities of discrete stochastic chemical reaction networks. *The Journal of chemical physics*, 132(3), 2010.

[31] Sheldon M Ross. *Introductory statistics.* Academic Press, 2017.

[32] Andrea Saltelli, Marco Ratto, Stefano Tarantola, and Francesca Campolongo. Sensitivity analysis for chemical models. *Chemical reviews*, 105(7):2811–2828, 2005.

[33] Peter Schuster. *Stochasticity in processes*. Springer, 2016.

[34] Patrick W Sheppard, Muruhan Rathinam, and Mustafa Khammash. Spsens: a software package for stochastic parameter sensitivity analysis of biochemical reaction networks. *Bioinformatics*, 29(1):140–142, 2013.

[35] Il'ya Meerovich Sobol'. On sensitivity estimation for nonlinear mathematical models. *Matematicheskoe modelirovanie*, 2(1):112–118, 1990.

[36] Tamás Turányi. Sensitivity analysis of complex kinetic systems. tools and applications. *Journal of mathematical chemistry*, 5(3):203–248, 1990.

[37] Judit Zádor, I Gy Zsely, and Tamás Turányi. Local and global uncertainty analysis of complex chemical kinetic systems. *Reliability Engineering & System Safety*, 91(10-11):1232–1240, 2006.